



Ultrasound irradiation effect on morphological and adsorptive properties of a nanoscale 3D Zn-coordination polymer and derived oxide

Lyara Ferreira Pereira^{a,1}, Allana Christina de Oliveira Frós^{a,1},
Milena Kowalczyk Manosso Amorim^b, Fernando Hallwass^a, Luciano Costa Almeida^c,
Bráulio Silva Barros^{d,*}, Joanna Kulesza^{a,*}

^a Universidade Federal de Pernambuco, Departamento de Química Fundamental, Av. Jornalista Anibal Fernandes, Cidade Universitária, 50740-560 Recife, PE, Brazil

^b Universidade Federal de Pernambuco, Centro de Ciências Exatas e da Natureza (CCEN), Programa de Pós-graduação em Ciência de Materiais, Av. Jornalista Anibal Fernandes, Cidade Universitária, 50740-560 Recife, PE, Brazil

^c Universidade Federal de Pernambuco, Departamento de Engenharia Química, Rua Artur de Sá, Cidade Universitária, 50740-521 Recife, PE, Brazil

^d Universidade Federal de Pernambuco, Departamento de Engenharia Mecânica, Av. da Arquitetura, Cidade Universitária, 50740-550 Recife, PE, Brazil

ARTICLE INFO

Keywords:

Ultrasound
MOF synthesis
Controlled morphology
Enhanced adsorption
BTEX

ABSTRACT

In this work, Zn-based coordination polymer $[Zn_2(1,3\text{-}bdc)\text{bzim}_2]_n$ was successfully synthesized by the sonochemical method using a 13 mm probe-type ultrasound operating at 20 kHz and amplitudes of 30, 40 and 50% corresponding to an acoustic power of 5.5, 8.6, and 10.3 W, respectively. Additionally, a sample was prepared by the slow-diffusion method for comparison. The samples were characterized by FTIR, PXRD, SEM, and BET techniques. The influence of the time and sonication amplitude on the yield of the reaction, crystallite size, and morphology were also studied. It was found that the sonochemical method provided the desired product in 83.9% within 20 min of sonication using the highest level of sonication amplitude. Moreover, this approach resulted in regular, controlled morphology, smaller particles, and higher surface area of the Zn-sample and derived oxide, than the slow diffusion method. The samples prepared by different methodologies were tested for the adsorption of BTEX (benzene, toluene, ethylbenzene, and xylenes) components in six different systems, and the uptakes were quantified by ^{13}C NMR spectroscopy. Both samples showed excellent adsorption of benzene, 119.8 mmol/g, and 88.1 mmol/g, for the coordination polymers prepared via the sonochemical and slow-diffusion methods, respectively, corresponding to 63.9%, and 46.9%. These results are in agreement with the non-polar surface of these samples.

1. Introduction

Metal-Organic Frameworks (MOFs), a class of coordination polymers, are highly advantageous in many applications such as catalysis, adsorption, gas separation, and storage, among others [1]. Tunable pore size and structural diversity are just two of the intriguing features that have made them attractive materials for researchers all over the world. Since synthesis conditions greatly affect the properties of these materials, it is of high importance to select a suitable synthesis method that leads to samples with desirable structure and morphology [2].

MOFs can be obtained in a simple way by the slow diffusion or solvothermal methods besides some alternative approaches such as mechanochemical [3], electrochemical [4,5], sonochemical [6], and microwave-assisted [7] methods. Compared to the routes

mentioned above, the sonochemical method stands out as one of the most advantageous approaches for MOFs preparation [8]. The application of high-energy ultrasound radiation is responsible for the process called acoustic cavitation in which rapid formation, growth, and collapse of bubbles called cavities takes place. In such conditions, the crystallization nuclei are immediately formed, leading to small and uniform crystallites of MOF material [2]. Thus, the sonochemical method often leads to smaller and more uniform particle sizes than other methodologies.

Furthermore, phase-purity and selectivity have been often reported [9]. Moreover, the parameters such as power and time of sonication may tune the morphology of the samples [10]. Nanostructures of Zn-based MOF from microspheres to uniform nanocubes have been prepared by varying the ultrasound power and time of reaction [11].

* Corresponding authors.

E-mail addresses: braulio.barros@ufpe.br (B. Silva Barros), joanna.kulesza@ufpe.br (J. Kulesza).

¹ Authors have an equivalent contribution.

Numerous papers have revealed the benefits of the sonochemical preparation of MOFs. Often, these materials present enhanced catalytic [12] and adsorptive properties [13–15] compared to their conventionally obtained samples mainly because of the higher surface area promoted by ultrasound irradiation.

The adsorption is one of the most efficient methods for the removal and recovery of harmful volatile organic compounds (VOCs), and Metal-Organic Frameworks stand on the top of the list of the used materials [16]. Benzene, toluene, ethylbenzene, and the isomers of xylene (*o*-, *m*-, and *p*-xylene) form a group of aromatic volatile organic compounds widely known as BTEX. The importance of these compounds in the industry is well recognized; they are used as raw materials to produce other chemical compounds, solvents, paints, among others [17]. However, because of their potential acute toxicity and health hazard to humans and aquatic life, BTEX are one of the most studied to be efficiently adsorbed and recovered. The recovery of BTEX from wastewaters is essential; however, most of the researchers deal with the adsorption from the gaseous phase. Thus, adsorption studies from the liquid phase are still needed, and the investigation of efficient and selective adsorbents for BTEX components are crucial.

Due to this scenario, herein, we report for the first time a simple, efficient, and reproducible sonochemical preparation of a Zn-MOF with the chemical formula of $[\text{Zn}_2(1,3\text{-bdc})(\text{bzim})_2]_n$. This material was previously prepared by our group via solvothermal [18] and electrochemical [5] methods, and its structure is depicted in Fig. 1. The obtained materials were tested for the adsorption of benzene, toluene, ethylbenzene, and xylenes (BTEX) from the liquid phase and showed remarkable uptake of benzene. The results were compared to a sample prepared by conventional slow diffusion method and zinc oxides derived from Zn-MOF samples. The relationship between structure/morphology and adsorption properties was established. Moreover, we present here a simple way to estimate the surface polarity of solid materials by ^{13}C NMR spectroscopy.

2. Experimental

2.1. Materials

All reagents and solvents were used as received without further purification. Isophthalic acid ($\text{C}_8\text{H}_6\text{O}_4$, 1,3- H_2bdc , 99%) and benzimidazole ($\text{C}_7\text{H}_6\text{N}_2$, Hbzim, 98%) were acquired from Sigma Aldrich. Zn ($(\text{CH}_3\text{COO})_2 \cdot 2\text{H}_2\text{O}$ ($\text{ZnAc}_2 \cdot 2\text{H}_2\text{O}$); and solvents: dimethylformamide (DMF), ethanol (EtOH) were purchased from Vetec. CDCl_3 (99.9% deuterated) and 1,4-dioxane (99.0%) for NMR analyses were purchased from Sigma Aldrich. For the adsorption tests, the solvents benzene (C_6H_6), toluene (C_7H_8), and xylene mixture (C_8H_{10}) were purchased from Vetec; *o*-xylene, *m*-xylene, *p*-xylene and ethylbenzene were

acquired from Sigma Aldrich. The commercial xylene mixture used in this work consisted of the mixture of four compounds, namely: *o*-xylene (*oX*, 2.7%), *m*-xylene (*mX*, 17.7%), *p*-xylene (*pX*, 8.5%) and ethylbenzene (EB, 71.1%), as verified by ^{13}C NMR spectroscopy and published in our previous paper [19].

2.2. Synthesis

2.2.1. Preparation of Zn-MOFs

Sonochemical syntheses of Zn-MOFs were carried out using an ultrasonic processor SONICS Vibra-Cell model VC 505 (500 W) equipped with a 13 mm titanium alloy probe, operating at 20 kHz of frequency and amplitudes of 30, 40 and 50% corresponding to an acoustic power of 5.5, 8.6, and 10.3 W, respectively. The acoustic power (P_{acous}) was determined by a calorimetric procedure based on the temperature rise of the liquid under ultrasonic irradiation [20]. In a typical experiment, 10 mL of water, 10 mL of ethanol, and 10 mL of DMF were mixed in a beaker of 50 mL and irradiated by ultrasound for 5 min. The temperature rise was measured every 10 s and plotted as a function of time. The slope of this curve was used in Eq. (1) to calculate the acoustic power in Watts for each amplitude studied.

$$P_{\text{acous}} = mC_p \frac{dT}{dt} \quad (1)$$

where m is the mass of the liquid (g), C_p is the specific heat capacity of the medium ($\text{J}\cdot\text{g}^{-1}\cdot^\circ\text{C}^{-1}$), and dT/dt is the slope of the temperature–time curve plotted ($^\circ\text{C}\cdot\text{s}^{-1}$). The mass of the liquid is the sum of the mass of 10 mL of water (10 g), 10 mL of ethanol (7.48 g), and 10 mL of DMF (9.49 g). The specific heat capacity of the medium depends on the proportion of each component (water, ethanol, and DMF) and can be calculated from volume according to Eq. (2).

$$C_p(\text{medium}) = \left(\frac{V_{\text{water}}}{V_{\text{total}}} \right) C_p(\text{water}) + \left(\frac{V_{\text{ethanol}}}{V_{\text{total}}} \right) C_p(\text{ethanol}) + \left(\frac{V_{\text{DMF}}}{V_{\text{total}}} \right) C_p(\text{DMF}) \quad (2)$$

where V_{total} is the sum of the volumes of water, ethanol, and DMF.

First, two solutions were prepared; $\text{ZnAc}_2 \cdot 2\text{H}_2\text{O}$ (4 mmol) in 10 mL of distilled water (solution 1) and solution 2 containing 2 mmol of 1,3- H_2bdc and 4 mmol of Hbzim dissolved in EtOH (10 mL) and DMF (10 mL). An ultrasound probe was immersed in the second solution placed in a 50 mL beaker, whereas the first solution was transferred to the dropping funnel. Then, the ultrasound irradiation was initiated in a sequence of pulses 6 s on, and 4 s off. Simultaneously, the metal salt solution was dropped slowly to the reaction mixture for 3 min. The ultrasound amplitude and the time of reaction were varied according to Table 1. At the end of the reaction, the ultrasound irradiation was turned off, and the white suspension of the product was centrifuged at

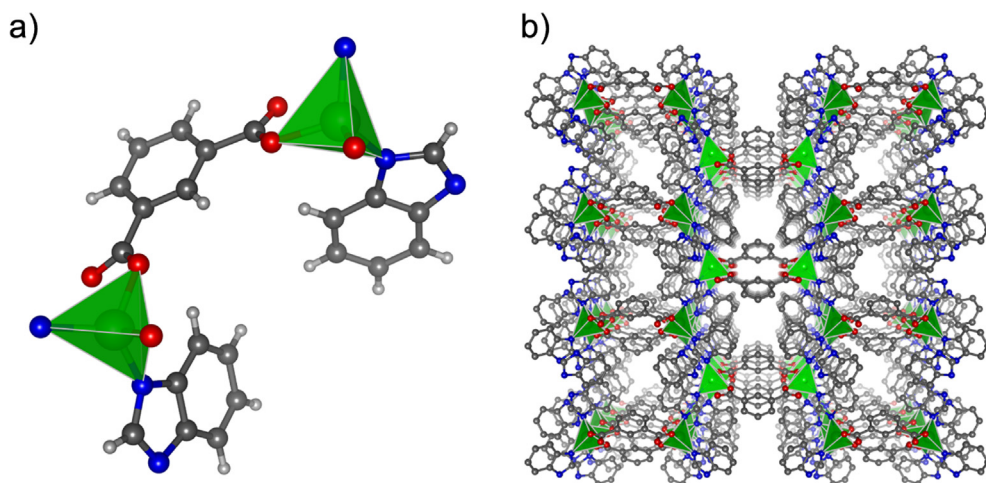


Fig. 1. a) Coordination environment around Zn^{2+} cations and b) Perspective view along the a -axis of the partially expanded framework of $[\text{Zn}_2(1,3\text{-bdc})(\text{bzim})_2]_n$ without hydrogen atoms. Color code: zinc (green), nitrogen (blue), oxygen (red), carbon (dark grey), hydrogen (light grey). (For interpretation of the references to colour in this figure legend, the reader is referred to the web version of this article.)

Table 1
Synthesis conditions (ultrasound amplitude and time), the yield of reaction, and the crystallite size of the prepared Zn-MOF samples.

Zn-MOF sample	Amplitude (%)	Time of sonicationT (min)	Yield of reaction (%)	Crystallite size (nm)
P30T20	30	20	77.5	19.9
P30T30	30	30	81.3	22.7
P50T20	50	20	83.9	19.5
P50T30	50	30	81.6	21.8
P40T25	40	25	81.6	21.6
SD	–	20 days	75.4	33.0
ST ^a	–	8 days	45.4	72.1
EC ^b	–	120 min	87.0	32.3
HT ^c	–	8.5 days	23.0	nd

nd – not determined.

^a Barros et al. [18].

^b Neto et al. [5].

^c Cui et al. [21].

5000 rpm, washed with DMF, and distilled water. Subsequently, the powder was dried in an oven at 90 °C for 2 h.

For comparison, the Zn-MOF was obtained by the slow-diffusion method at room temperature according to the previously reported procedure [18] with minor modifications. The two solutions of the same concentrations as for the sonochemical method were mixed under stirring for about ten minutes and then left standing at room temperature for 20 days. After that time, the obtained white powder was treated as described for the sonochemical method. The product was named as SD.

2.2.2. Synthesis of ZnO

The Zn-MOF samples P50T20 and SD were heated at a rate of 5 °C/min in the air to 850 °C, and held at this temperature for 2 h, resulting in samples ZnO_P50T20_2h and ZnO_SD_2h, respectively. Moreover, the sample P50T20 was also thermolyzed at 850 °C for 1 h, and the derived oxide was denominated as ZnO_P50T20_1h. The temperature was chosen based on our previous TGA results [18].

2.3. Characterization

Powder X-ray diffraction patterns were recorded on a Bruker D2 Phaser using CuK_α (λ = 1.5406 Å) radiation with Ni filter, at voltage 30 kV and 10 mA. Experiments were conducted at 2θ values ranging from 5 to 50° with a step of 0.02°. The crystallite sizes of samples were estimated using the Scherrer equation using the two most intense peaks of the PXRD patterns at around 2θ = 7.8° and 9.4°. The simulated PXRD pattern was obtained using the program Mercury 3.8. Fourier transform infrared (ATR-FTIR) experiments were carried out on a Bruker Vertex 70/v spectrometer at the range of 4000–400 cm⁻¹. Morphological analyses and images were acquired on a Scanning Electron Microscopy (SEM), model Tescan Mira 3. The samples P50T20, SD, ZnO_P50T20_2h, and ZnO_SD_2h were characterized for their pore properties with nitrogen adsorption/desorption at liquid nitrogen

Table 2
The quantity of BTEX components used in six tested systems (A–F).

System/composition (mL)	Benzene	Toluene	Ethylbenzene	<i>o</i> -xylene	<i>m</i> -xylene	<i>p</i> -xylene
A*	–	–	–	–	–	–
B*	–	0.5	–	–	–	–
C*	0.5	–	–	–	–	–
D*	0.5	0.5	–	–	–	–
E	0.3	0.3	–	–	–	–
F	0.2	0.2	0.2	0.2	0.2	0.2

*system includes 0.5 mL of commercial xylene mixture (ethylbenzene, *o*-xylene, *m*-xylene and *p*-xylene).

temperature (77 K) in a Quantachrome adsorption apparatus model NovaWin2 and the surface area was determined by BET and BJH methods. Before starting N₂ adsorption/desorption measurements, the samples were degassed in situ at 200 °C for 3 h.

2.4. NMR measurements

¹³C NMR spectra were acquired in an NMR spectrometer Agilent 400 MHz at 298 K in 5 mm NMR tube. CDCl₃ was used as a solvent and internal chemical shift reference. ¹³C longitudinal relaxation times (T₁) were measured using the standard Inversion-Recovery pulse sequence. qNMR spectra were acquired with a spectral width of 23.6 kHz, the acquisition time of 1.39 s, 32 k memory data points, interpulse delay of 50 s (5 × highest T₁ value), excitation pulse of 45° and 16 transients. To eliminate NOE effects, the decoupler was gated on only during acquisition. The signal integrations were computed according to the GSD protocol [22] using Mnova 11.04 software.

2.5. BTEX adsorption tests

The sonochemically-prepared sample with the highest yield and smallest crystallite size (P50T20) and the sample prepared by slow diffusion (SD), both previously dried overnight at 200 °C, were used in adsorption tests of BTEX (benzene, toluene, ethylbenzene, xylenes) in a liquid phase at room temperature. BTEX uptake was evaluated in competitive adsorption experiments for six different solution compositions, which are listed in Table 2. For systems A–D, a total of 0.5 mL of the commercial mixture (EB, *o*-x, *m*-x, *p*-x) was used.

In an adsorption test, 30 mg of the adsorbent were put in contact without stirring with the BTEX solution of the known composition for 2 h. After this time, the supernatant solution was withdrawn immediately and transferred to 5 mm NMR tube, 0.3 mL of CDCl₃ were added, and the ¹³C qNMR spectrum was acquired. In parallel, blank experiments were also conducted by using BTEX solutions without adsorbent for all systems and were analyzed under the same conditions as the adsorption solutions. The quantification method of the BTEX adsorption by ¹³C qNMR has been elaborated by our group and published in our previous paper [19].

The quantity of each component (in mols) adsorbed on the materials was calculated according to Eq. (3):

$$n_{adsorbed} = \frac{\Delta I_x N_y}{I_y N_x} n_y \quad (3)$$

where ΔI_x equal to I_{x1} – I_{x2} is the difference between the integrals from one signal of component x before the adsorption (blank experiment without adsorbent, Spectrum 1) and after adsorption (adsorption experiment, Spectrum 2), and N_x is the number of the carbons in the molecule of x present in this signal. In the same way, I_y is integral from one signal of the component y, which has a known concentration in the solution (used as a reference for the quantification), n_y is the number of mols of component y, and N_y is the number of the carbons in the molecule of y present in this signal. All formula deduction may be found in our previous paper [19]. Initially, 1,4-dioxane was used as a reference for quantification in all studied systems to verify the adsorption uptake

of each component from the solution. Because ethylbenzene, present in the xylene, was not adsorbed from the systems A-D, it was then used as a reference for the quantification. 1,4-dioxane was used as a reference for quantification in systems E and F.

For comparison, zinc oxide samples ZnO_P50T20 and ZnO_SD were tested in adsorption from system B.

All adsorption experiments were done in triplicate, and the integral area corresponds to the average of the integrals measured ten times. Some examples of the recorded ^{13}C NMR spectra are placed in SI.

2.6. Surface polarity estimation

The surface polarity of the MOF samples (P50T20 and SD) was estimated based on quantitative ^{13}C NMR spectroscopic measurements of liquid-phase adsorption. The surface polarity was characterized through the adsorption uptake of two different solvents of opposite polarity, hexane, and *N,N*-dimethylformamide (DMF), whereas 1,4-dioxane was used as a reference for quantification. 20 mg of the previously dried sample were immersed in a mixture of hexane (0.3 mL) and DMF (0.3 mL) for 2 h. After this time, the supernatant solution was withdrawn immediately, placed in a 5 mm NMR tube and diluted with 0.3 mL of CDCl_3 and 0.3 mL of 1,4-dioxane. Soon after, the ^{13}C qNMR spectrum was acquired. The quantification procedure was the same as described for BTEX adsorption tests. The example of ^{13}C NMR spectra before and after adsorption of DMF and hexane are placed in SI (Fig. S1).

The quantity of DMF and hexane adsorbed on the materials in competitive adsorption experiments in the liquid phase was calculated according to the Eq. (4). The surface polarity (SP) corresponds to the affinity of the adsorbent towards polar (DMF, $\mu = 3.82$) or nonpolar (hexane, $\mu = 0.00$) solvent and was expressed as a ratio of adsorption % of DMF and hexane as follows:

$$SP = \frac{\%DMF}{\%hexane} \quad (4)$$

3. Results and discussion

3.1. Synthesis

The yields of the sonochemical syntheses were good and comparable to each other, with an average yield of 81.2%. Some syntheses were repeated, and in each case, the pure-phase product was obtained with the reaction yield around 81%, what indicates the repeatability and reproducibility of the sonochemical method. Moreover, this method is more efficient than slow diffusion (75.4%), solvothermal (45.4%) [18], and hydrothermal (23.0%) [21] approaches in terms of the yield and time of reaction. Slightly higher reaction yield achieved through electrochemical synthesis at room temperature (EC) [5] can be explained by longer reaction time than any sonochemical syntheses. It seems that the amplitude of ultrasound irradiation and the time of reaction did not have a significant influence on the reaction yield, indicating the efficiency and reproducibility of this method. However, the lowest yield was observed in the case of sample P30T20, for which the lowest amplitude and the shortest reaction time of sonication were used.

3.2. FTIR

Fig. 2 shows the FTIR spectra of the samples prepared under ultrasound irradiation and slow-diffusion sample compared to the spectrum of the ligand 1,3- H_2bdc . All spectra are similar, suggesting the formation of the same structure independently of the synthesis method used. Thus, different synthesis parameters (reaction time and ultrasound amplitude) did not affect the formation of the product, indicating the reproducibility of this method. The FTIR spectra are practically

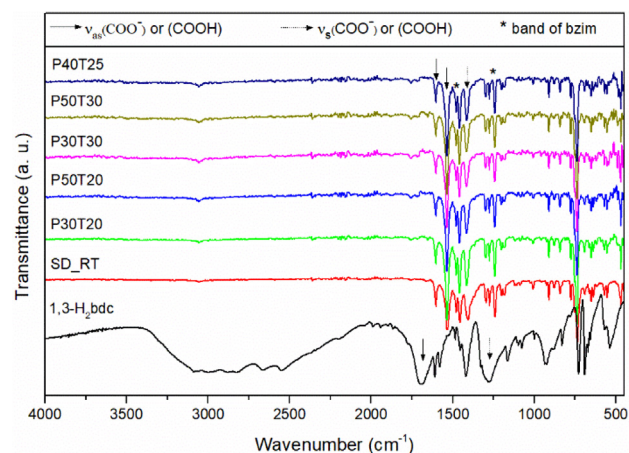


Fig. 2. FTIR spectra of Zn-MOF samples prepared by slow-diffusion and sonochemical methods compared to the spectrum of the ligand 1,3- H_2bdc .

identical to those previously reported by our group for samples prepared by solvothermal [18], and electrochemical [5] methods. The absence of bands in the region $1680\text{--}1730\text{ cm}^{-1}$ indicates the complete deprotonation of COOH groups and the coordination of the carboxylate groups to the zinc center. Strong bands at around 1604 and 1537 cm^{-1} and 1407 cm^{-1} corresponding to the stretching, asymmetric and symmetric modes of COO^- also indicate the formation of COO-Zn coordination bonds. The bands at around 1477 and 1243 cm^{-1} , attributed to the vibrations of the aromatic ring and stretching vibration ν (C-N) of benzimidazole, respectively are also visible confirming the presence of benzimidazole in the structure what is in agreement with the expected structure for $[\text{Zn}_2(1,3\text{-bdc})(\text{bzim})_2]_n$ [18,21] of these samples. No bands corresponding to the solvents present in the structures may be observed.

3.3. PXRD

The PXRD patterns of coordination polymers prepared by ultrasound irradiation and slow-diffusion methods match well with the simulated pattern of $[\text{Zn}_2(1,3\text{-bdc})(\text{bzim})_2]_n$ [21], and no additional peaks are observed, what confirms the formation of a phase pure product (Fig. 3).

Samples prepared by the sonochemical route present broader diffraction peaks than that obtained via a slow diffusion method indicating

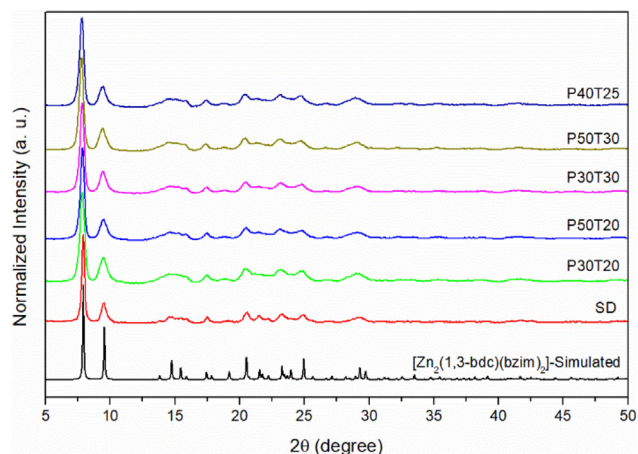


Fig. 3. PXRD patterns of samples obtained by sonochemical method (under different synthesis conditions) and slow-diffusion method compared to the simulated pattern calculated from the single crystal data of $[\text{Zn}_2(1,3\text{-bdc})(\text{bzim})_2]_n$ [21].

smaller crystallite sizes of these samples, which is in agreement with the calculated values based on the PXRD patterns (Table 1). The average crystallite sizes of samples produced under ultrasound irradiation were uniform (21.1 ± 1.6 nm) and smaller than of those prepared by conventional methods (solvothermal and slow-diffusion at room temperature, 72.1 [18] and 33.0 nm, respectively). Compared to traditional synthetic techniques, the sonochemical approach is more convenient, reproducible, and controllable. Sample SD prepared by the slow diffusion method at room temperature shows a similar average crystallite size to the recently reported sample prepared by the electrochemical approach [5] at room temperature (33.0 vs. 32.3 nm).

The thermolysis of P50T20 (for 1 and 2 h) and SD (for 2 h) led to the formation of pure zinc oxides based on PXRD patterns (Fig. S6). The diffraction peaks of the three patterns match well with the simulated pattern of ZnO (COD CIF file no 9004180). No secondary crystalline phases were observed.

3.4. SEM

The micrographs of the representative MOF samples prepared by the sonochemical (P50T20) and slow diffusion (SD) methods and their respective zinc oxides are shown in Fig. 4. Both MOF samples present morphology in the form of agglomerates of plate-like particles; however, the sample prepared *via* the sonochemical method presents smaller, regular, and more uniform in size particles (Fig. 4a), whereas the slow-diffusion sample consists of larger, irregular plates (Fig. 4b). The SEM images of the rest of the samples obtained under ultrasound irradiation were very similar, indicating that the amplitude and time of sonication did not have a significant influence on the morphology of the samples. Thus, the sonochemical approach is a reproducible method for

the preparation of this MOF material.

The synthesis method affected the morphology not only of the MOF samples but also their respective oxides. The SEM image of the zinc oxide prepared from sonochemically-synthesized MOF presents spherical and uniform particles (Fig. 4c), whereas the calcination of the MOF obtained via slow diffusion method led to the highly agglomerated and pre-sintered ZnO particles (Fig. 4d).

Both micrographs of ZnO_P50T20_1h and ZnO_P50T20_2h (Fig. S7) exhibits particles with some coalescence, suggesting that a sintering process has initiated during calcination. Particle size histograms of obtained ZnO samples show that calcination of MOF P50T20 at 850 °C during 2 h promotes particle growth, when compared with ZnO particles obtained after 1 h of thermolysis (Fig. 5). Also, ZnO obtained after 2 h of thermolysis shows a wider distribution of particle size.

3.5. BET

Both MOF samples (P50T20 and SD) show a reversible Type-II isotherm of N₂ adsorption/desorption which is typical for a macroporous adsorbent [23] (Fig. 6) and a BET (BJH) surface area of 41.59 (44.68) and 5.80 (7.59) m².g⁻¹, for P50T20 and SD, respectively. The values are low, but one can see that the sonochemically prepared MOF sample presents seven times higher surface area than the sample prepared by the slow diffusion method. Moreover, the surface area of P50T20 is almost three times higher than of the previously reported sample prepared by the electrochemical method [5]. These results also indicate the benefits of sonochemically-assisted synthesis of MOFs.

As expected, the BET surfaces areas of ZnO samples were much lower than for Zn-MOF samples (1.58 and 0.58 cm³/g) for ZnO_P50T20_2h and ZnO_SD_2h, respectively.

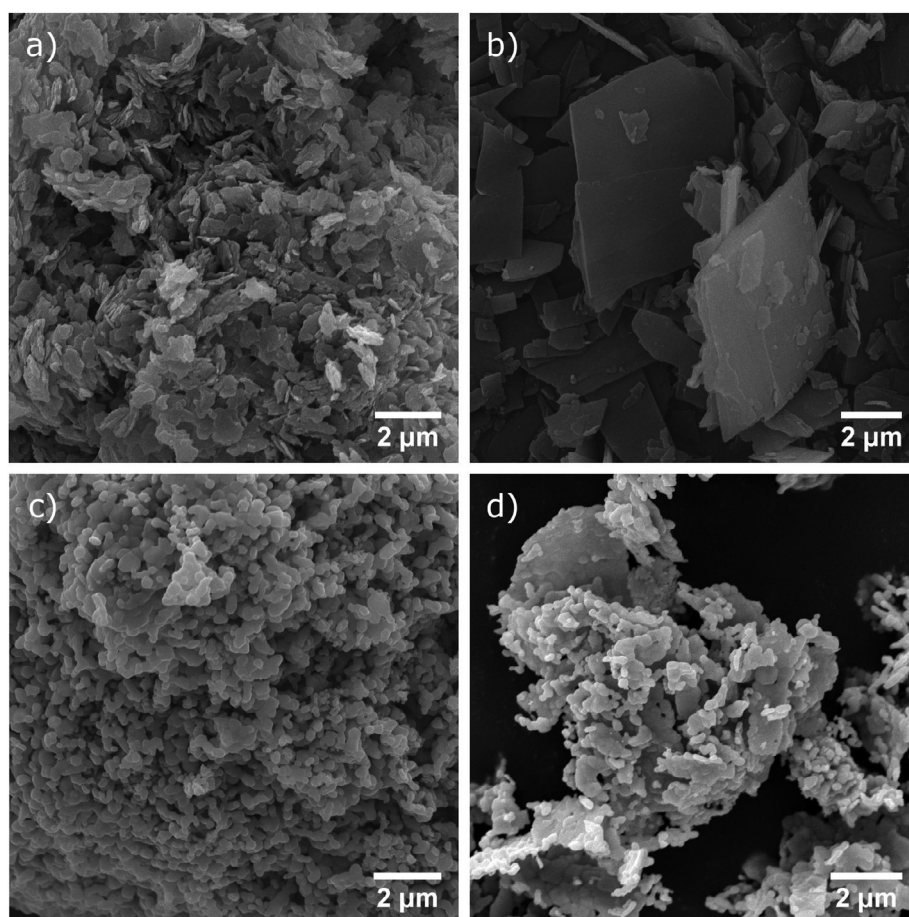


Fig. 4. SEM images of the Zn-MOF samples prepared by a) sonochemical, b) slow-diffusion methods, and derived oxides c) ZnO_P50T20_2h and d) ZnO_SD_2h.

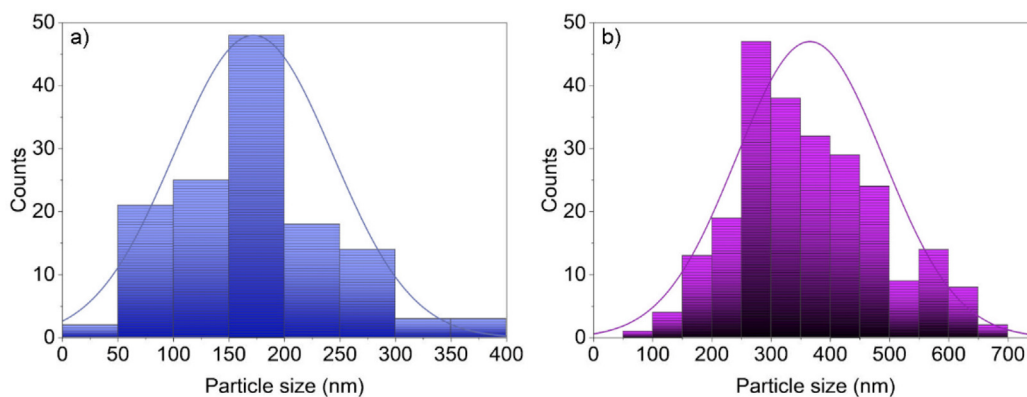


Fig. 5. Particle size histograms for ZnO samples obtained after a) 1 h and b) 2 h of thermolysis of sonochemically-prepared MOF (P50T20).

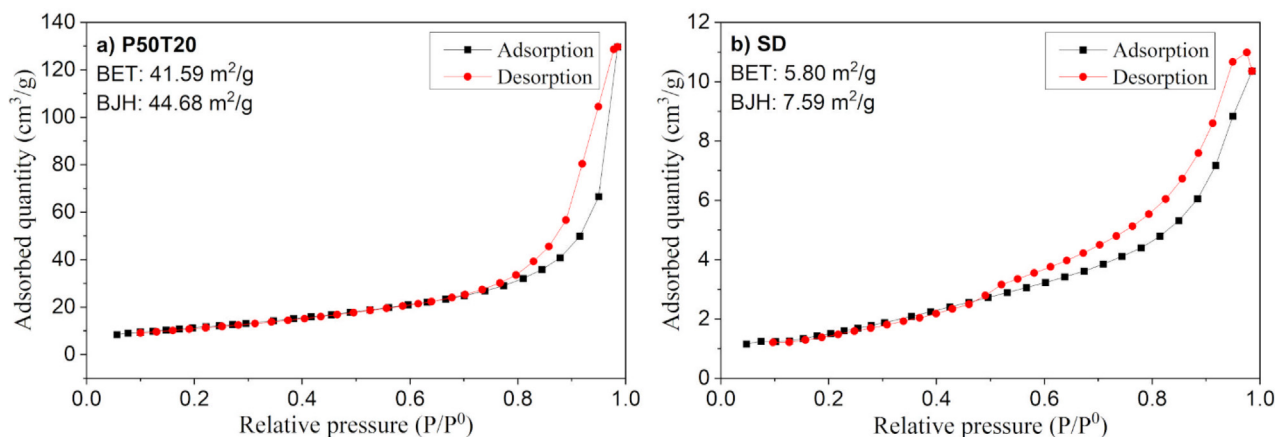


Fig. 6. N_2 adsorption-desorption isotherms of the MOF samples prepared by a) sonochemical (P50T20) and b) slow diffusion method (SD).

3.6. Adsorption

The percentage of volatile compounds adsorption on samples prepared by sonochemical (P50T20) and slow-diffusion (SD) methods are shown in Fig. 7.

Both samples show a preference for the least abundant xylene component in system A, *o*-xylene, 23.6, and 16.4% for P50T20 and SD, respectively. However, in the case of P50T20, *m*-xylene and *p*-xylene uptakes are similar and almost the same (21.5 and 21.4%). The *m*-xylene and *p*-xylene adsorption capacity of the slow-diffusion sample is almost three times lower (6.1 and 8.3, respectively) than for sonochemically prepared sample.

On the other hand, when toluene is present in a solution (system B), *o*-xylene is the least adsorbed component for both samples (2.7%). In this case, toluene is preferentially adsorbed with 59.2 and 22.3%, for P50T20 and SD, respectively. Regarding xylene components, the adsorption preference follows the same order for both samples: *p*X (14.6 and 8.3%) > *m*X (7.2 and 6.4%) > *o*X (2.7 and 2.7%), although, sonochemically-prepared sample is more efficient, mainly for *p*-xylene adsorption.

Both samples show selectivity for benzene with 63.9 and 46.9% of the adsorption for P50T20 and SD, respectively for system C. Among xylene components, the adsorption uptake is maintained in the same order: *p*X (20.3 and 11.7%) > *m*X (13.5 and 8.2%) > *o*X (6.4 and 3.6%), with higher efficiency of the sonochemically-prepared sample. In the competitive adsorption with toluene and benzene (system D), both samples show a preference for benzene with 36.9 and 32.2% for P50T20 and SD, respectively. Regarding xylene components, the adsorption order is as follows: *p*X (16.6 and 14.0%) > *m*X (14.7 and 10.8%) > *o*X (6.4 and 0.0%). Toluene adsorption is relatively low,

0.461, and 0.186 mmol/g, corresponding to 9.8 and 4.0%, for P50T20 and SD, respectively.

In the equivolume system E, both adsorbents show a preference for benzene with similar quantities adsorbed (72.5 vs. 68.2%) for P50T20 and SD, respectively. Sonochemically prepared sample adsorbs around 2.2 times more benzene than toluene, whereas the difference is even higher for room-temperature prepared sample (three times more benzene adsorbed than toluene).

When all BTEX components were present in a solution in equivolume amounts (system F), both samples exhibit a preference for benzene 58.6 and 49.9%, for P50T20 and SD, respectively. The adsorption of toluene was also high, corresponding to 42.1 and 34.1%, respectively. Among xylene components, the adsorption uptakes are maintained in the same order: *p*X (18.2 and 13.7%) > *m*X (17.0 and 12.8%) = *o*X (17.0 and 12.8%).

The adsorption affinity of $[Zn_2(1,3\text{-}bdc)\text{bzim}_2]_n$ for C_8H_{10} molecules generally follows the same order for all systems studied: *p*-xylene > *m*-xylene > *o*-xylene > ethylbenzene, except for the system A. Ethylbenzene was not adsorbed from any of the systems, what can be explained by the larger size of the molecule (EB 6.625 Å × 5.285 Å × 9.361 Å) than other BTEX components (*o*X: 7.269 Å × 3.834 Å × 7.826 Å; *m*X: 8.994 Å × 3.949 Å × 7.315 Å; *p*X: 6.618 Å × 3.810 Å × 9.146 Å) [24]. Additionally, the bulky lateral chain of ethylbenzene can cause a steric hindrance and hamper the surface interactions with the adsorbents.

It is worth noting that both samples show a preference for benzene (systems C, D, E, F) and *p*-xylene (although less pronounced) among xylene isomers (for systems B, C, D, F), both non-polar molecules, what is in agreement with the apolar surface of the adsorbents based on the surface polarity estimation tests (SP = 0.17 and 0.14 for P50T20 and

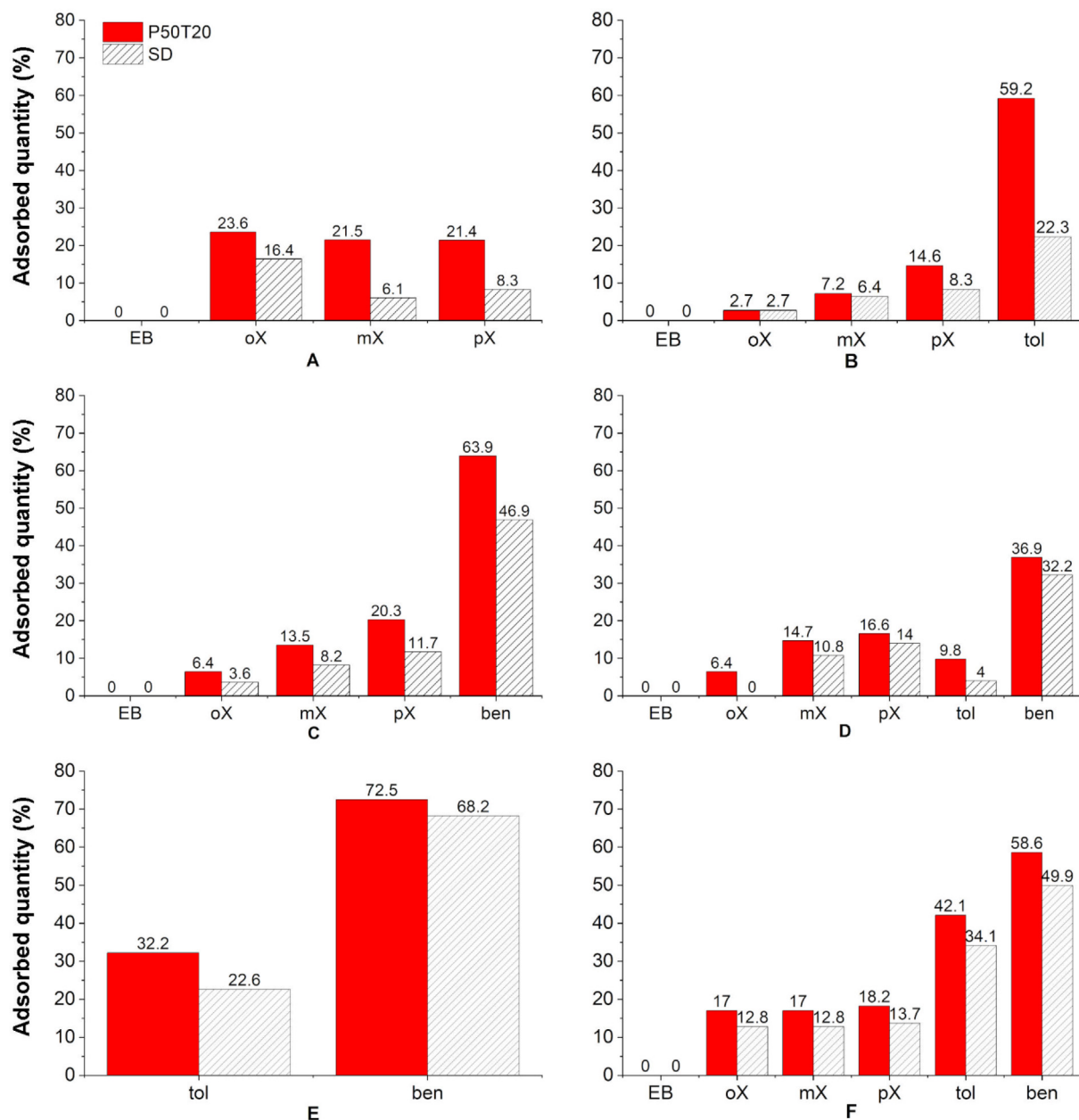


Fig. 7. Comparison of the quantity of the adsorbed BTEX components in different systems on Zn-MOFs prepared by the sonochemical and slow-diffusion method.

SD, respectively (see details in SI). The overall adsorption capacity is higher for the sample prepared by the sonochemical method, which was already expected since the surface area of P50T20 is seven times higher than of SD (41.59 and $5.80 \text{ m}^2 \text{ g}^{-1}$, respectively).

The derived oxides ZnO_P50T20_2h and ZnO_SD_2h were tested for the adsorption in system B (Fig. 8).

As for the MOF samples, oxides did not adsorb ethylbenzene. Interestingly, oxide derived from sonochemically-prepared MOF, ZnO_P50T20_2h show similar adsorption profile $\text{tol} > \text{px} > \text{mx} > \text{ox} > \text{EB}$ to the pristine MOF, although with much lower adsorption uptake (up to 14.4%) and poor selectivity. On the other hand, ZnO_SD_2h shows selectivity for *m*-xylene (24.0%), followed by *p*-xylene, *o*-xylene, and toluene. Different affinities of both ZnO samples may be associated with the morphology of both ZnO adsorbents. The general lower adsorption uptake for oxides compared to pristine MOFs can be related to the lower surface area and weaker interactions between the inorganic adsorbents and organic molecules.

BTEX adsorption on ZnO are very rare in the literature, and most of

the studies use modified ZnO samples [25,26]. For example, Salehi et al. reported toluene adsorption from aqueous solution ($c = 5 \text{ mg.L}^{-1}$) on the nano-ZnO sample prepared by a three-stage method: precipitation, surface modification, and polymer grafting. The authors found the maximum uptake of 12.8 mg.g^{-1} (0.14 mmol.g^{-1}) at pH 6 and contact time of 30 min [27]. As expected, this value is much lower than that obtained for our ZnO samples due to the low concentration of toluene in the tested solution.

The adsorption affinities for BTEX of presented here Zn-MOFs are different than of our recently reported calixarene-based molecular Zn-coordination network calix-TAA-Zn [19]. The presence of calixarene in the structure combined with the hydrophobic surface of the material enhanced the selectivity for *p*-xylene among xylene isomers [19]. Such behavior is not recognized in the case of presented here Zn-MOFs for which no significant distinction was observed between xylenes (system A). On the other hand, P50T20 and SD are much more efficient for the adsorption of benzene (system C: 119.8 and 88.1 mmol/g , respectively; system D: 69.33 and 60.40 mmol/g , respectively) or toluene from

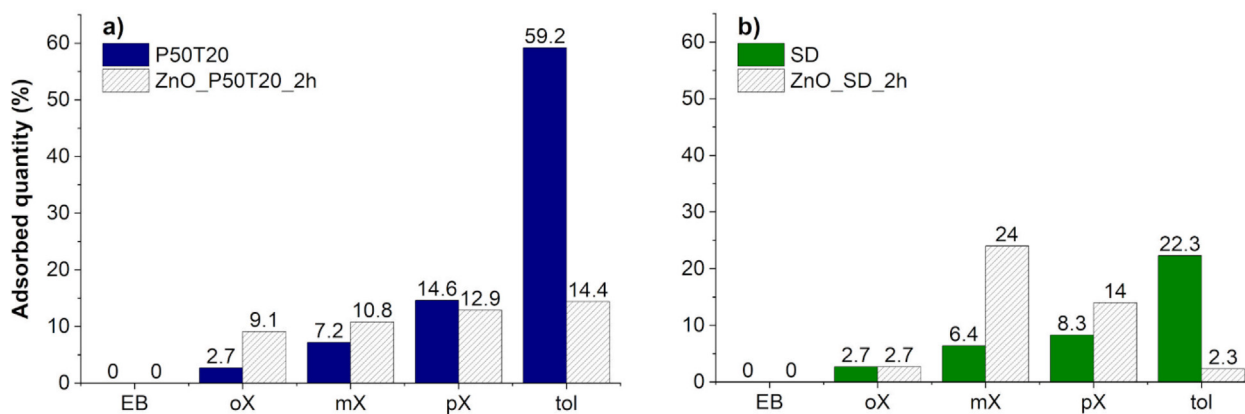


Fig. 8. Comparison of the quantity of the adsorbed BTEX components in system B on Zn-MOFs and derived oxides.

system B (92.70 and 35.00 mmol/g, respectively) than calix-TAA-Zn (system C: 38.33 mmol/g of benzene; system D: 15.27 mmol/g of benzene; system B: 13.33 mmol/g of toluene) [19].

To the best of our knowledge, studies of BTEX adsorption from the liquid phase are still rare, and very few papers have been published [28]. Most of the published works refer to the uptake of gaseous compounds, which makes it difficult to compare with our data. The excellent amount of liquid benzene adsorbed on Zn-MOFs is much higher than for reported MOFs like MIL-101(Cr), 16.7 mmol/g [29] and 16.4 mmol/g [30], MOF-520(Al), 12.9 mmol/g [31], MOF-5, 12.8 mmol/g [31], MOF-177, 10.24 mmol/g [32], ZIF-8, 7.3 mmol/g [31], MIL-125-NH₂, 4.06 mmol/g [33], Cu-3@MIL-101(Cr), 1.46 mmol/g [34], and other adsorbents, such as activated carbon (6.5 mmol/g) [35].

Also, the uptake of toluene by P50T20 (92.70 mmol/g for system B) is higher than by common MOFs such as MIL-101(Cr) (11.9 mmol/g) [30], HKUST-1 (9.42 mmol/g) [36], MOF-177 (6.35 mmol/g) [32], MIL-125-NH₂, 3.18 mmol/g [33], UiO-NH₂ (2.74 mmol/g) [35], ZIF-67 (2.43 mmol/g) [35], UiO-66, (1.96 mmol/g) [37], 1.80 mmol/g [35], 1.64 mmol/g [38], MOF-199 (1.73 mmol/g) [35], MIL-101(Fe) (1.07 mmol/g) [35], MOF-5 (0.36 mmol/g) [35], zeolites (4A Zeolite, 0.33 mol/g) [35], and activated carbon AC (6.5 mmol/g) [39].

The comparison can be also visualized in Fig. 9.

We also found that $[Zn_2(1,3-bdc)(bzim)_2]_n$ is chemically stable for at least 24 h contact with water (see details in SI). Therefore, the combination of the high adsorption capacity and water resistance makes this material a promising candidate for BTEX removal and/or separation from wastewaters. However, in such a case, lower uptake from a dilute aqueous mixture might be expected as the concentration is

a crucial factor in adsorption capacity.

4. Conclusions

A 3D Zn-coordination polymer based on isophthalate and benzimidazole mixed ligands $[Zn_2(1,3-bdc)(bzim)_2]_n$ was successfully synthesized by conventional slow-diffusion and sonochemical approaches. Effects of the sonication time and ultrasonic amplitude on the yield of the reaction, size of crystallites, and morphology were also investigated. The results were similar in all cases; however, the highest amplitude and the shortest time, provided the smallest size of crystallite and the highest yield. Representative samples of both methods adsorbed benzene preferentially what was in agreement with their non-polar surface estimated by ¹³C NMR method. The enhanced adsorption of the sonochemically-prepared sample compared to the slow-diffusion sample was associated with the seven-times higher surface area and regular plate-like morphology. Due to its high adsorption capacity and water resistance, this material is a promising candidate for BTEX removal and/or separation from wastewaters.

CRediT authorship contribution statement

Lyara Ferreira Pereira: Methodology, Investigation. **Allana Christina Oliveira Frós:** Methodology, Investigation, Validation. **Milena Kowalczyk Manosso Amorim:** Investigation, Visualization. **Fernando Hallwass:** Investigation, Formal analysis. **Luciano Costa Almeida:** Investigation, Formal analysis. **Bráulio Silva Barros:** Formal analysis, Resources, Writing - original draft, Visualization, Writing - review & editing. **Joanna Kulesza:** Supervision, Conceptualization,

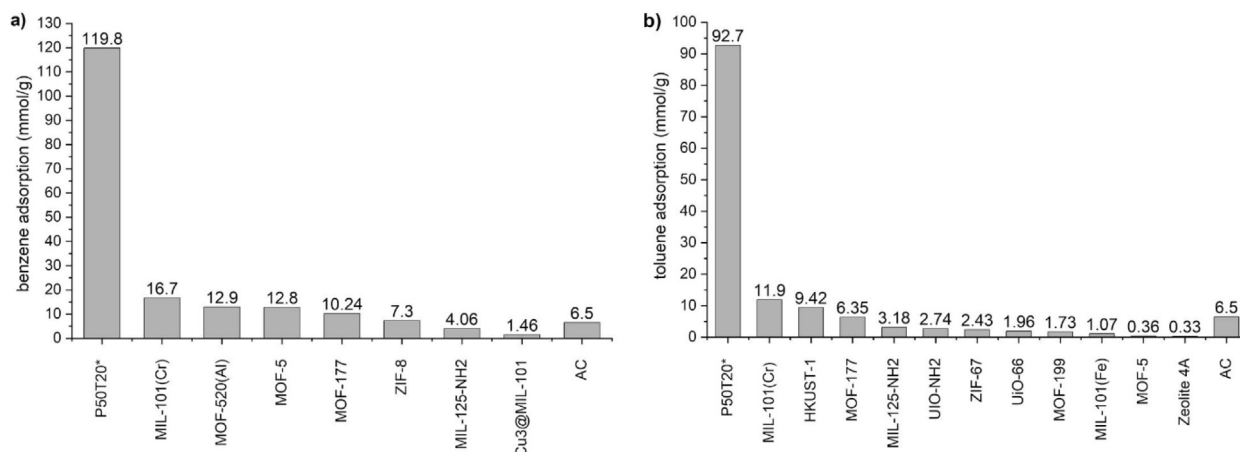


Fig. 9. Comparison of the quantity of benzene and toluene adsorbed on P50T20 and other literature materials. *adsorption from the liquid phase.

Resources, Writing - original draft.

Declaration of Competing Interest

The authors declare that they have no known competing financial interests or personal relationships that could have appeared to influence the work reported in this paper.

Acknowledgment

The students (L.F.P, A.C.O.F. and M.K.M.A.) thank CNPq for a scholarship granted. This work was financially supported by CNPq and FACEPE (Grants nos. 403747/2016-3, APQ-0818-1.06/15, APQ-0675-1.06/14). This study was financed in part by the Coordenação de Aperfeiçoamento de Pessoal de Nível Superior – Brasil (Capes) – Finance Code 001.

Appendix A. Supplementary data

Supplementary data to this article can be found online at <https://doi.org/10.1016/j.ultsonch.2020.105275>.

References

- [1] A.U. Czaja, N. Trukhan, U. Müller, Industrial applications of metal-organic frameworks, *Chem. Soc. Rev.* 38 (2009) 1284–1293, <https://doi.org/10.1039/b804680h>.
- [2] B.S. Barros, O.J. de Lima Neto, A.C. de Oliveira Frós, J. Kulesza, Metal-organic framework nanocrystals, *ChemistrySelect* 3 (2018) 7459–7471, <https://doi.org/10.1002/slct.201801423>.
- [3] M. Klimakow, P. Klobes, A.F. Thünemann, K. Rademann, F. Emmerling, Mechanochemical synthesis of metal-organic frameworks: a fast and facile approach toward quantitative yields and high specific surface areas, *Chem. Mater.* 22 (2010) 5216–5221, <https://doi.org/10.1021/cm1012119>.
- [4] J. Kulesza, B.S. Barros, I.M.V. Da Silva, G.G. Da Silva, S. Alves Júnior, Efficient and environmentally friendly electrochemical synthesis of the metallacalixarene [Cu(1,3-bdc)-DMF]·2H₂O, *CrystEngComm* 15 (2013) 8881–8882, <https://doi.org/10.1039/c3ce41679h>.
- [5] O.J. de Lima Neto, A.C. de O. Frós, B. Barros, A.F. de Farias Monteiro, J.E. Kulesza, Rapid and efficient electrochemical synthesis of a zinc-based nano-MOF for Ibuprofen adsorption, *New J. Chem.* 5 (2019) 5518–5524, <https://doi.org/10.1039/c8nj06420b>.
- [6] G.G. da Silva, C.S. Silva, R.T. Ribeiro, C.M. Ronconi, B.S. Barros, J.L. Neves, S.A. Júnior, Sonoelectrochemical synthesis of metal-organic frameworks, *Synth. Met.* 220 (2016) 369–373, <https://doi.org/10.1016/j.synthmet.2016.07.003>.
- [7] R. Vakili, S. Xu, N. Al-Janabi, P. Gorgojo, S.M. Holmes, X. Fan, Microwave-assisted synthesis of zirconium-based metal organic frameworks (MOFs): Optimization and gas adsorption, *Microporous Mesoporous Mater.* (2017), <https://doi.org/10.1016/j.micromeso.2017.10.028>.
- [8] C. Vaitis, G. Sourkouni, C. Argiris, Metal organic frameworks (MOFs) and ultrasound: a review, *Ultrason. Sonochem.* 52 (2019) 106–119, <https://doi.org/10.1016/j.ultsonch.2018.11.004>.
- [9] N.A. Khan, S.H. Jhung, Synthesis of metal-organic frameworks (MOFs) with microwave or ultrasound: rapid reaction, phase-selectivity, and size reduction, *Coord. Chem. Rev.* 285 (2015) 11–23, <https://doi.org/10.1016/j.ccr.2014.10.008>.
- [10] G. Sargazi, D. Afzali, A. Mostafavi, A novel synthesis of a new thorium (IV) metal organic framework nanostructure with well controllable procedure through ultrasound assisted reverse micelle method, *Ultrason. Sonochem.* 41 (2018) 234–251, <https://doi.org/10.1016/j.ultsonch.2017.09.046>.
- [11] V. Safarifar, A. Morsali, Facile preparation of nanocubes zinc-based metal-organic framework by an ultrasound-assisted synthesis method; precursor for the fabrication of zinc oxide octahedral nanostructures, *Ultrason. Sonochem.* 40 (2018) 921–928, <https://doi.org/10.1016/j.ultsonch.2017.09.014>.
- [12] M. Joharian, A. Morsali, Ultrasound-assisted synthesis of two new fluorinated metal-organic frameworks (F-MOFs) with the high surface area to improve the catalytic activity, *J. Solid State Chem.* 270 (2019) 135–146, <https://doi.org/10.1016/j.jssc.2018.10.046>.
- [13] M.Y. Masoomi, M. Bagheri, A. Morsali, Porosity and dye adsorption enhancement by ultrasonic synthesized Cd(II) based metal-organic framework, *Ultrason. Sonochem.* 37 (2017) 244–250, <https://doi.org/10.1016/j.ultsonch.2017.01.018>.
- [14] M.Y. Masoomi, M. Bagheri, A. Morsali, High adsorption capacity of two Zn-based metal-organic frameworks by ultrasound assisted synthesis, *Ultrason. Sonochem.* 33 (2016) 54–60, <https://doi.org/10.1016/j.ultsonch.2016.04.013>.
- [15] R. Abazari, A.R. Mahjoub, Ultrasound-assisted synthesis of Zinc(II)-based metal organic framework nanoparticles in the presence of modulator for adsorption enhancement of 2,4-dichlorophenol and amoxicillin, *Ultrason. Sonochem.* 42 (2018) 577–584, <https://doi.org/10.1016/j.ultsonch.2017.12.027>.
- [16] X. Li, L. Zhang, Z. Yang, P. Wang, Y. Yan, J. Ran, Adsorption materials for volatile organic compounds (VOCs) and the key factors for VOCs adsorption process: a review, *Sep. Purif. Technol.* 235 (2020) 116213, <https://doi.org/10.1016/j.seppur.2019.116213>.
- [17] M. Heydari, S. Sabbaghi, S. Zeinali, Adsorptive removal of toluene from aqueous solution using metal-organic framework MIL-101(Cr): removal optimization by response surface methodology, *Int. J. Environ. Sci. Technol.* 16 (2019) 6217–6226, <https://doi.org/10.1007/s13762-019-02214-9>.
- [18] B.S. Barros, J. Chojnacki, A.A. Macêdo Soares, J. Kulesza, L. Lourenço Da Luz, S.A. Júnior, Thermostability and photophysical properties of mixed-ligand carboxylate/benzimidazole Zn(II)-coordination polymers, *Mater. Chem. Phys.* 162 (2015) 364–371, <https://doi.org/10.1016/j.matchemphys.2015.05.079>.
- [19] A.C. de Oliveira Frós, M.A. de Oliveira, A.A. Macêdo Soares, F. Hallwass, J. Chojnacki, B.S. Barros, S.A. Júnior, J. Kulesza, Selective adsorption of BTEX on calixarene-based molecular coordination network determined by ¹³C NMR spectroscopy, *Inorg. Chim. Acta* 492 (2019) 161–166, <https://doi.org/10.1016/J.ICA.2019.04.031>.
- [20] R.F. Contamine, A.M. Wilhelm, J. Berlan, H. Delmas, Power measurement in sonochemistry, *Ultrason. – Sonochem.* 2 (1995) S43–S47, [https://doi.org/10.1016/1350-4177\(94\)00010-P](https://doi.org/10.1016/1350-4177(94)00010-P).
- [21] Y.-C. Cui, J.-J. Wang, B. Liu, G.-G. Gao, Q.-W. Wang, Poly[μ₄-benzene-1,3-di-carboxylato-di-μ₂-benzimidazolato-dizinc(II)], *Acta Crystallogr. Sect. E Struct. Reports Online* 63 (2007) m1204–m1205, <https://doi.org/10.1107/S1600536807013712>.
- [22] M.A. Bernstein, S. Sýkora, C. Peng, A. Barba, C. Cobas, Optimization and automation of quantitative NMR data extraction, *Anal. Chem.* 85 (2013) 5778–5786, <https://doi.org/10.1021/ac400411q>.
- [23] K.S.W. Sing, D.H. Everett, R.A.W. Haul, L. Moscou, R.A. Pierotti, J. Rouquerol, T. Siemienińska, Reporting physisorption data for gas/solid systems with special reference to the determination of surface area and porosity, *Pure Appl. Chem.* 57 (1985) 603–619, <https://doi.org/10.1351/pac198557040603>.
- [24] C.E. Webster, R.S. Drago, M.C. Zerner, Molecular dimensions for adsorptives, *J. Am. Chem. Soc.* 120 (1998) 5509–5516, <https://doi.org/10.1021/ja973906m>.
- [25] J. Zeng, C. Zhao, F. Chong, Y. Cao, F. Subhan, Q. Wang, J. Yu, M. Zhang, L. Luo, W. Ren, X. Chen, Z. Yan, Oriented ZnO nanorods grown on a porous polyaniline film as a novel coating for solid-phase microextraction, *J. Chromatogr. A* 1319 (2013) 21–26, <https://doi.org/10.1016/j.chroma.2013.10.040>.
- [26] X. Hu, C. Wang, R. Luo, C. Liu, J. Qi, X. Sun, J. Shen, W. Han, L. Wang, J. Li, Double-shelled hollow ZnO/carbon nanocubes as an efficient solid-phase microextraction coating for the extraction of broad-spectrum pollutants, *Nanoscale* 11 (2019) 2805–2811, <https://doi.org/10.1039/c8nr09180c>.
- [27] J. Al-Sabahi, T. Bora, M. Al-Abri, J. Dutta, Efficient visible light photocatalysis of benzene, toluene, ethylbenzene and xylene (BTEX) in aqueous solutions using supported zinc oxide nanorods, *PLoS One* 12 (2017) 1–16, <https://doi.org/10.1371/journal.pone.0189276>.
- [28] R. Navarro Amador, L. Cirre, M. Carboni, D. Meyer, BTEX removal from aqueous solution with hydrophobic Zr metal organic frameworks, *J. Environ. Manage.* 214 (2018) 17–22, <https://doi.org/10.1016/j.jenvman.2018.02.097>.
- [29] Z.L.Z. Zhao, X. Li, S. Huang, Q. Xia, Adsorption and diffusion of benzene on chromium-based metal organic framework MIL-101 synthesized by microwave irradiation, *Ind. Eng. Chem. Res.* 50 (2011) 2254–2261, <https://doi.org/10.1021/ie101414n>.
- [30] K. Yang, Q. Sun, F. Xue, D. Lin, Adsorption of volatile organic compounds by metal-organic frameworks MIL-101: Influence of molecular size and shape, *J. Hazard. Mater.* 195 (2011) 124–131, <https://doi.org/10.1016/j.jhazmat.2011.08.020>.
- [31] S. Gwardiak, B. Szcześniak, J. Choma, M. Jaroniec, Benzene adsorption on synthesized and commercial metal-organic frameworks, *J. Porous Mater.* 26 (2019) 775–783, <https://doi.org/10.1007/s10934-018-0678-0>.
- [32] K. Yang, F. Xue, Q. Sun, R. Yue, D. Lin, Adsorption of volatile organic compounds by metal-organic frameworks MOF-177, *J. Environ. Chem. Eng.* 1 (2013) 713–718, <https://doi.org/10.1016/j.jece.2013.07.005>.
- [33] B. Kim, Y.R. Lee, H.Y. Kim, W.S. Ahn, Adsorption of volatile organic compounds over MIL-125-NH₂, *Polyhedron* 154 (2018) 343–349, <https://doi.org/10.1016/j.poly.2018.08.010>.
- [34] D. Wang, G. Wu, Y. Zhao, L. Cui, C.H. Shin, M.H. Ryu, J. Cai, Study on the copper (II)-doped MIL-101(Cr) and its performance in VOCs adsorption, *Environ. Sci. Pollut. Res.* 25 (2018) 28109–28119, <https://doi.org/10.1007/s11356-018-2849-6>.
- [35] K. Vellingiri, P. Kumar, A. Deep, K.H. Kim, Metal-organic frameworks for the adsorption of gaseous toluene under ambient temperature and pressure, *Chem. Eng. J.* 307 (2017) 1116–1126, <https://doi.org/10.1016/j.cej.2016.09.012>.
- [36] Z. Zhao, S. Wang, Y. Yang, X. Li, J. Li, Z. Li, Competitive adsorption and selectivity of benzene and water vapor on the microporous metal organic frameworks (HKUST-1), *Chem. Eng. J.* 259 (2015) 79–89, <https://doi.org/10.1016/j.cej.2014.08.012>.
- [37] T.K. Vo, V.N. Le, V.C. Nguyen, M. Song, D. Kim, K.S. Yoo, B.J. Park, J. Kim, Microwave-assisted continuous-flow synthesis of mixed-ligand UiO-66(Zr) frameworks and their application to toluene adsorption, *J. Ind. Eng. Chem.* 86 (2020) 178–185, <https://doi.org/10.1016/j.jiec.2020.03.001>.
- [38] X. Zhang, X. Lv, X. Shi, Y. Yang, Y. Yang, Enhanced hydrophobic UiO-66 (University of Oslo 66) metal-organic framework with high capacity and selectivity for toluene capture from high humid air, *J. Colloid Interface Sci.* 539 (2019) 152–160, <https://doi.org/10.1016/j.jcis.2018.12.056>.
- [39] D. Saha, N. Miranda, A. Levchenko, Liquid and vapor phase adsorption of BTX in lignin derived activated carbon: Equilibrium and kinetics study, *J. Clean. Prod.* 182 (2018) 372–378, <https://doi.org/10.1016/j.jclepro.2018.02.076>.